






Initial beam emission spectroscopy diagnostic system on HL-2A tokamak

Cite as: Rev. Sci. Instrum. **89**, 10D122 (2018); <https://doi.org/10.1063/1.5039350>

Submitted: 07 May 2018 . Accepted: 22 August 2018 . Published Online: 08 October 2018

R. Ke , Y. F. Wu , G. R. McKee, Z. Yan, K. Jaehnig, M. Xu, M. Kriete , P. Lu, T. Wu, L. A. Morton , X. Qin , X. M. Song, J. Y. Cao, X. T. Ding, and X. R. Duan

COLLECTIONS

Paper published as part of the special topic on [Proceedings of the 22nd Topical Conference on High-Temperature Plasma Diagnostics](#)

Note: Paper published as part of the Proceedings of the 22nd Topical Conference on High-Temperature Plasma Diagnostics, San Diego, California, April 2018.



View Online



Export Citation



CrossMark

ARTICLES YOU MAY BE INTERESTED IN

[Fast ion D-alpha measurements using a bandpass-filtered system on EAST](#)

Review of Scientific Instruments **89**, 10D121 (2018); <https://doi.org/10.1063/1.5038828>

[Simultaneous measurement of C VI, Ne X, and Li III charge exchange lines on EAST](#)

Review of Scientific Instruments **89**, 10D119 (2018); <https://doi.org/10.1063/1.5036835>

[The beam emission spectroscopy diagnostic on the DIII-D tokamak](#)

Review of Scientific Instruments **70**, 913 (1999); <https://doi.org/10.1063/1.1149416>

Lock-in Amplifiers
up to 600 MHz



Watch



Initial beam emission spectroscopy diagnostic system on HL-2A tokamak

R. Ke,^{1,2,a)} Y. F. Wu,^{2,3,4} G. R. McKee,³ Z. Yan,³ K. Jaehnig,³ M. Xu,² M. Kriete,³ P. Lu,² T. Wu,² L. A. Morton,³ X. Qin,³ X. M. Song,² J. Y. Cao,² X. T. Ding,² and X. R. Duan²

¹Department of Engineering Physics, Tsinghua University, Beijing 100084, China

²Center for Fusion Science, Southwestern Institute of Physics, Chengdu, Sichuan 610041, China

³Department of Engineering Physics, University of Wisconsin-Madison, Madison, Wisconsin 53706-1687, USA

⁴School of Physics, University of Science and Technology of China, Hefei, Anhui 230026, China

(Presented 16 April 2018; received 7 May 2018; accepted 22 August 2018;
 published online 8 October 2018)

A beam emission spectroscopy system is being developed and deployed on the HL-2A tokamak to measure local low wavenumber ($k_{\perp}\rho_i < 1$) density fluctuations by measuring the Doppler-shifted emission from a 50 kV deuterium heating neutral beam. High spatial resolution ($\Delta r \leq 1$ cm, $\Delta z \leq 1.5$ cm) measurements are achieved with customized in-vacuum optics. High frequency, high-gain preamplifiers sample the light intensity at a Nyquist frequency of 1 MHz and achieve a high S/N ratio via high optical throughput, low-noise preamplifiers, and high quantum efficiency photodiodes. A first set of 16 detector channels [configured in an 8 (radial) \times 2 (poloidal) array] has been installed and tested at HL-2A, covering the radial range $r/a = 0.8$ – 1.1 . The frequency and wavenumber spectra have been measured under different plasma conditions. Initial measurements have demonstrated the capability of measuring edge plasma density fluctuation spectra and the poloidal flow velocity fields with a high S/N ratio. *Published by AIP Publishing.* <https://doi.org/10.1063/1.5039350>

I. INTRODUCTION

Understanding typical turbulent fluctuations and the resulting transport is one of the key scientific issues for predicting and optimizing the performance of magnetically confined fusion devices. A new beam emission spectroscopy (BES) diagnostic system^{1,2} is being developed and deployed on the HL-2A tokamak to measure low wavenumber ($k_{\perp}\rho_i < 1$) density fluctuations. The BES diagnostic system is a widely deployed 2D measurement tool in tokamaks^{1–7} and stellarator devices;⁸ it measures density fluctuations in the edge and core regions. Atoms in the neutral beam are collisionally excited via collisions with ions and electrons. The fluorescence is emitted when the excited atoms are subsequently de-excited by spontaneous emission or collisional de-excitation. By measuring the intensity of the Doppler-shifted neutral beam D_{α} emission, the local plasma density fluctuations can be calculated as

$$\frac{\tilde{I}}{I} = K(T_e, n_e, \dots) \frac{\tilde{n}_e}{n_e}, \quad (1)$$

where K is the coefficient that depends weakly on local plasma parameters,⁹ $\frac{\tilde{n}_e}{n_e}$ is the normalized electron density fluctuations, and $\frac{\tilde{I}}{I}$ is the relative light intensity fluctuations. This measurement of density fluctuations provides measurements of turbulence spectra, radial/poloidal correlation lengths, turbulence decorrelation times, time-resolved velocity field, and 2D turbulence imaging. These measurements contribute greatly to the study of core and edge turbulence, pedestal dynamics and instabilities, as well as energetic particle physics and magnetohydrodynamic (MHD) instabilities.

Note: Paper published as part of the Proceedings of the 22nd Topical Conference on High-Temperature Plasma Diagnostics, San Diego, California, April 2018.

^{a)} Author to whom correspondence should be addressed: kerui@swip.ac.cn.

In this paper, the newly designed BES system on the HL-2A tokamak is introduced in Sec. II and preliminary fluctuation measurements are presented in Sec. III, with a discussion in Sec. IV.

II. THE BES DIAGNOSTIC SYSTEM ON HL-2A

HL-2A is a middle-size tokamak device with major radius $R = 1.65$ m and minor radius $a = 0.4$ m. A variety of auxiliary heating sources have been deployed, including electron cyclotron resonance heating (ECRH), lower-hybrid current drive (LHCD), and neutral beam injection (NBI). The BES optical viewing system is installed on the port to the left of (clockwise from) the neutral beam (Fig. 1). This neutral beam consists of four 50 keV deuterium sources that inject tangentially near the mid-plane in the direction of the plasma current. BES observes the red-shifted D_{α} emission near $\lambda \approx 659$ nm [Fig. 1(e)].

The optical system viewing the beam emission is installed inside the vacuum chamber and consists of an $f/1.65$, 280-mm-focal-length objective lens which includes a 10 cm field lens in the tilt tube (Fig. 2). The 18 cm diameter objective lens images the beam emission from the radial range $0.2 < r/a < 1.1$ of the plasma. The optical axis of the front-end objective lens elements is offset from the optical axis of the field lens to optimize throughput. This design allows the first objective lens element to be closer to the beam while ensuring that the optical system can be installed in the limited space with sufficient spatial coverage. The BES port is located below the mid-plane and is tilted upwards by $\sim 9^{\circ}$ relative to the equatorial plane, consistent with the HL-2A magnetic field pitch angle range of 5° – 9° . This design optimizes spatial resolution by viewing tangent to the local magnetic field lines. The beam line is

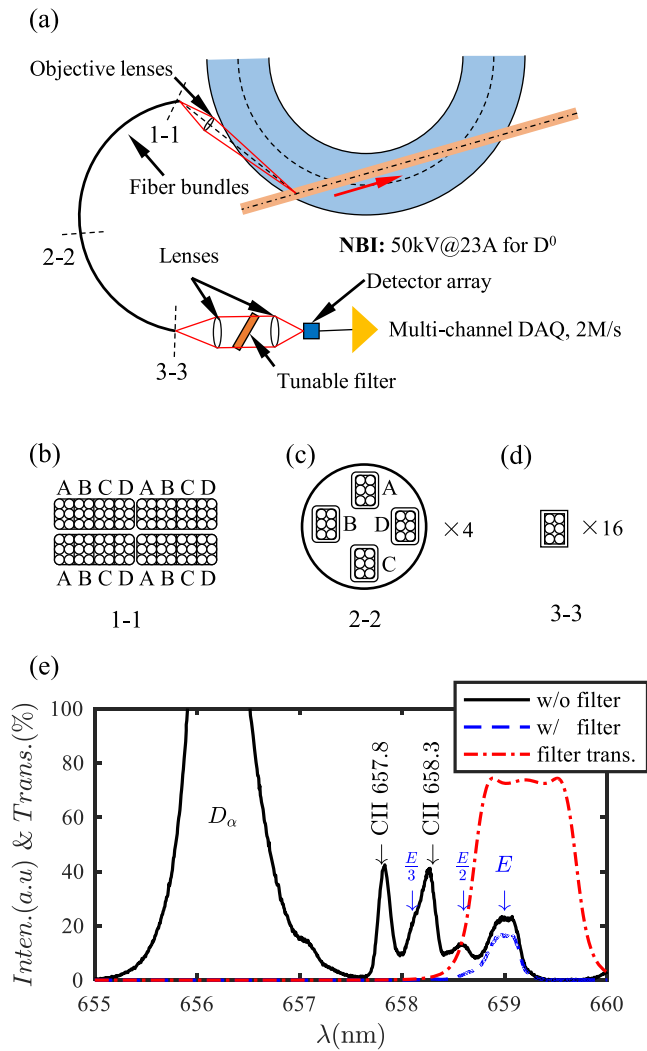


FIG. 1. Schematic of the BES system on the HL-2A tokamak. (a) Layout of the BES system (top view). (b) Arrangement of fibers on the image end [image plane, see cross section 1-1 in (a)]. Each channel contains 6 fibers (2×3 array), and 4 radially offset channels (A, B, C, and D) form one unit. (c) Layout of fiber bundles in one unit [cross section 2-2 in (a)]. (d) Arrangement of fibers on the detector end [cross section 3-3 in (a)]. (e) Beam emission intensity (black solid line), filtered beam emission intensity (blue dashed line), and the filter transmission (red dotted-dashed line).

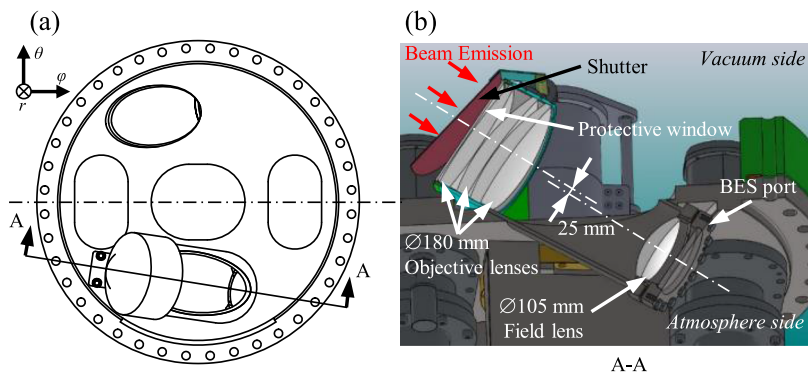


FIG. 2. Design of the optical lens of the HL-2A BES system. (a) 600 mm diameter mid-plane flange (as viewed from the vacuum side). The BES port is the lowest one (BES shutter and other diagnostics installed on this window are not shown for simplicity), with the optical axis tilted upwards by $\sim 9^\circ$. (b) Design of the BES objective lens [cross section A-A in (a)]. The axis of the 180 mm diameter objective lens is offset by 25 mm from the axis of the 105 mm diameter field lens, which is installed inside the tilted tube. The objective lens is protected by a flat 3 mm thick window at the front of the lenses. A mechanical shutter can be closed to protect the optics when not in use. A 105 mm diameter, 12 mm thick quartz glass window forms the air-vacuum interface.

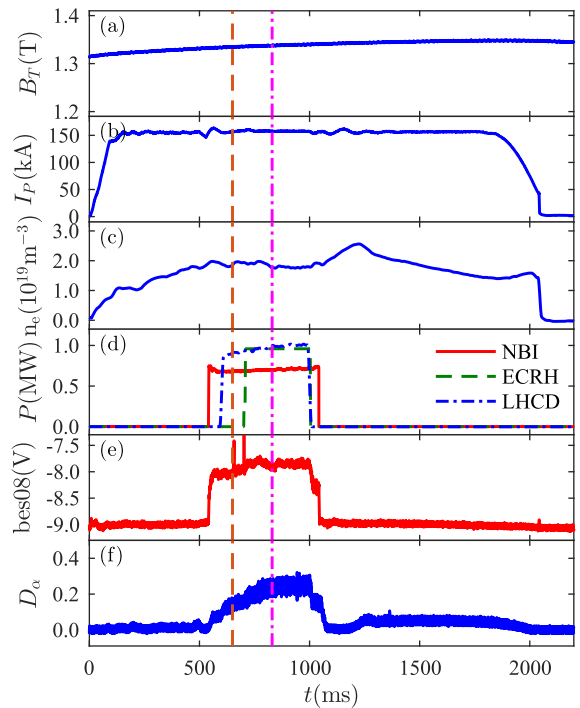


FIG. 3. One shot on HL-2A discharge with multiple auxiliary heating sources. Time evolution of (a) toroidal field $B_T \sim 1.33$ T, (b) plasma current $I_p \sim 150$ kA, (c) line-averaged electron density $n_e \sim 1 \sim 2 \times 10^{19} \text{ m}^{-3}$, (d) auxiliary heating power of NBI (red solid line), ECRH (green dashed line), and LHCD (blue dotted-dashed line), (e) one of the BES channels located at $\rho \sim 0.85$, and (f) D_α emission intensity in the divertor.

focused to a curved image surface that is located just outside a vacuum window to allow fiber access. The vacuum window is integrated into the optical design. A flat 3 mm thick (changeable) protective window is located closest to the plasma at the front of the objective lens elements, and a mechanical shutter protects the optical system when not in use.

A 10 m fiber bundle array is located outside the vacuum chamber at the image plane of the objective optical system (Fig. 1). Each channel consists of 6 1-mm-diameter fibers that are arranged as a 2×3 fiber array (2 in the radial direction and 3 in the poloidal direction). 4 channels are grouped together in a 1 (poloidal) \times 4 (radial) configuration [Fig. 1(b) shows 4

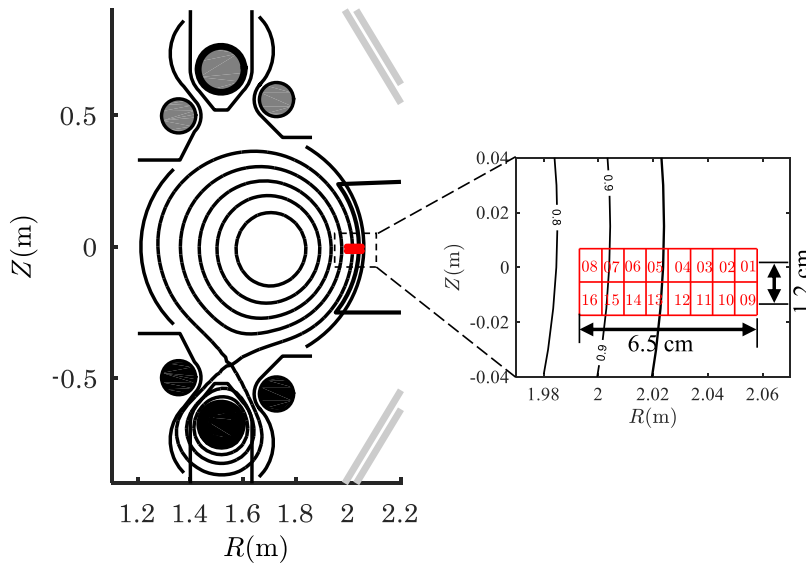


FIG. 4. An arrangement of BES channels for edge/SOL turbulence experiments. 16 channels are deployed in an 8 (radial) \times 2 (poloidal) 2D array on the outer midplane.

such units]. Currently, there are 4 units available on the HL-2A tokamak. The configuration of 4 units is flexible. Figure 1(b) shows a typical scheme of a 2×2 configuration that has been initially deployed [i.e., the 16 channels are configured in an 8 (radial) \times 2 (poloidal) array]. This design increases the radial resolution without losing much flexibility. In each unit, the front face of the four channels are arranged like staircases (not shown) to match the curved image plane.

The red-shifted beam emission is relayed to the collimating lenses by the fiber bundle arrays. The collimated light passes through a customized interference filter (50 mm diameter) with 70% peak transmission in the wavelength range of 659.2–660.2 nm and <5% low transmission at 658.3 nm [where an undesired carbon II emission line exists, see Fig. 1(e)]. The filter is rotatable, enabling a slight shift in the transmission band. Then focusing lenses image the filtered light onto the PIN photodiode detectors.

A 2.65 mm square PIN photodiode (PPD) based high frequency, high gain, and low-noise detector array is used as the beam emission detector.¹⁰ The detector and its preamplifier circuit are chilled to -10°C in a vacuum chamber with a pressure of $4 \sim 10$ mTorr to minimize electronic noise and prevent any condensation. The black curve in Fig. 5 shows the total detector noise. Dark current (i -noise) dominates the noise spectra¹⁰ at low frequencies, while voltage noise (e -noise), which arises from the pre-amplifier, dominates the noise spectra¹⁰ at higher frequencies and increases monotonically with the frequency.

The detector electronics converts the light signal to a voltage signal, and then the voltage signal is recorded with a 2 Ms/s 14-bit D-TACQ digitizer (ACQ132). An FPGA-based fast-impulse-response digital filter is applied with a passband of 0–900 kHz to serve as an anti-alias filter.

III. PRELIMINARY FLUCTUATION MEASUREMENTS

The 16-channel BES system is currently being operated on the HL-2A tokamak. Figure 3 shows a typical L-mode discharge on HL-2A with multiple auxiliary heating sources, including 700 kW NBI, 1 MW ECRH, and 1 MW LHCD. The

plasma line-averaged density is $\sim 2 \times 10^{19} \text{ m}^{-3}$. An example BES signal (channel 8 near $r/a = 0.85$) in Fig. 3(e) demonstrates the response to the NBI. The BES arrangement is shown in Fig. 4. 16 BES channels are deployed as an 8 (radial) \times 2 (poloidal) 2D array at the outer mid-plane, focusing on the SOL and edge/pedestal region covering $r/a \sim 0.8 \sim 1.1$ (Fig. 4). The equilibrium is obtained from EFIT at 650 ms (see Fig. 3, brown vertical dashed line), and the last closed flux surface (LCFS) is located at $r = 37.4$ cm. The radial and poloidal spatial resolutions are 0.8 cm and 1.2 cm, respectively. Two time slices are chosen to demonstrate the density fluctuation measurements with BES: One is before the 1 MW ECRH is turned on (brown vertical dashed line in Fig. 3) and the other is when ECRH is on (magenta vertical dotted-dashed line in Fig. 3). The auto-power spectra of the BES signal measured by channel 16 are shown in Fig. 5. The background dark noise spectrum (black line in Fig. 5) has been subtracted; the plasma signals include plasma fluctuations and photon shot noise. The spectra indicate that BES achieves a bandwidth of up to

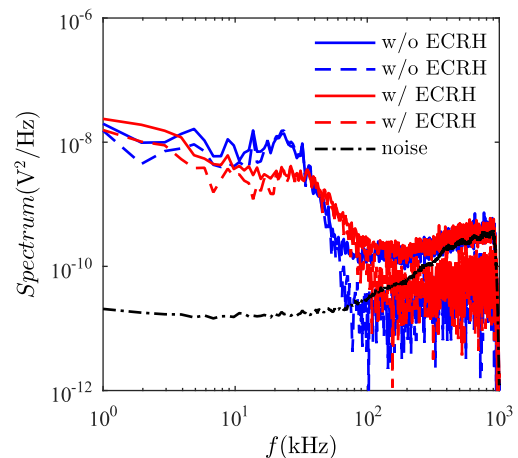


FIG. 5. Auto-spectra of detector noise (black dotted-dashed line) and raw BES signal without ECRH (blue, 640 ~ 660 ms, at the time indicated in Fig. 3 by a brown vertical dashed line) and with ECRH (red, 820 ~ 840 ms, at the time indicated in Fig. 3 by a magenta vertical dotted-dashed line). The blue/red dashed lines are the cross-power of two poloidally separated channels.

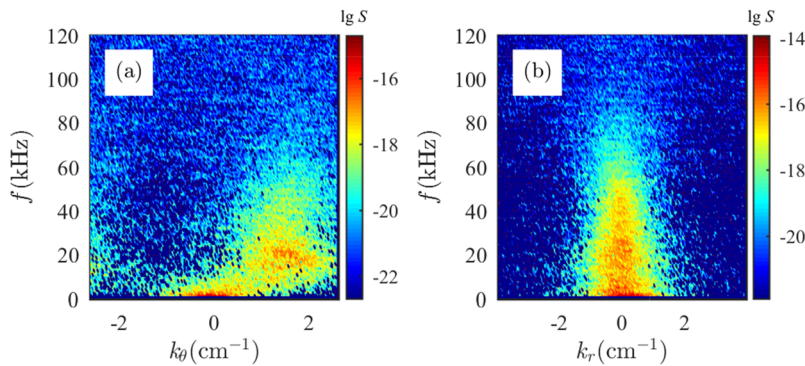


FIG. 6. k -spectra measured by two (a) poloidally separated and (b) radially separated BES channels.

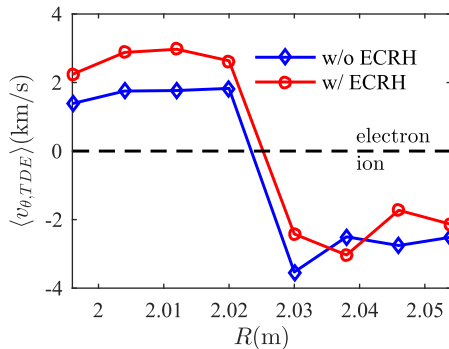


FIG. 7. Poloidal velocity measured by BES using the TDE method at 650 ms (blue squares) and 830 ms (red circles). The positive/negative values of $\langle v_{\theta,TDE} \rangle$ correspond to the electron/ion diamagnetic directions, respectively.

900 kHz with the digital anti-alias filter, which includes the frequency band where density fluctuations are typically dominant. When ECRH is on, the turbulence around $\rho \sim 0.85$ is shifted to a higher frequency due to a higher Doppler shift, which is consistent with the increasing poloidal rotation at this location (shown in Fig. 7) since the $E \times B$ velocity largely determines the fluctuation spectral range.

The 2D array enables us to perform correlation analysis in both poloidal and radial directions. Figure 6 shows the k -spectra measured by two poloidally separated [Fig. 6(a)] and radially separated [Fig. 6(b)] BES channels^{11–13} inside the LCFS. Turbulence with $|k_{\theta}| \leq 2.6 \text{ cm}^{-1}$ and $|k_r| \leq 4 \text{ cm}^{-1}$ is well resolved. The 20 ~ 80 kHz broadband turbulence has a wavenumber range of $0.8 \text{ cm}^{-1} \leq k_{\theta} \leq 2.1 \text{ cm}^{-1}$ and $-0.9 \text{ cm}^{-1} \leq k_r \leq 0.9 \text{ cm}^{-1}$ and propagates in the electron diamagnetic direction in the laboratory frame. The poloidal velocity can be measured utilizing time delay estimation (TDE) methods.^{14,15} Figure 7 shows the poloidal velocity profile measured by BES at 650 ms (w/o ECRH) and 830 ms (w/ECRH). The profiles demonstrate that the BES system is capable of measuring the edge poloidal flow evolution.

IV. DISCUSSION

An initial BES diagnostic system on HL-2A that consists of 16 spatial channels is capable of measuring the fre-

quency and wavenumber spectra of density fluctuations in the region of $r/a \sim 0.8$ -1.1 with a high S/N ratio, as well as the turbulence flow velocity evolution. Simultaneous measurements of density fluctuations in the core and edge regions are of great importance to transport studies, such as turbulence spreading, L-H transitions, and H-mode pedestal physics. The current fiber mount is designed to cover a wide radial range of the plasma cross section. Additional channels are being fabricated and will be deployed in the future to extend the capability of this imaging BES diagnostic system.

ACKNOWLEDGMENTS

The authors would like to thank the HL-2A group for their extensive support. This work is supported by the National Natural Science Foundation of China under Grant Nos. 11575055, 11705052, 11375053, and 11475056, the International S&T Cooperation program of China under Grant No. 2015DFA61760, the Chinese National Fusion Project for ITER under Grant Nos. 2014108000 and 2015104000, Contract No. 15CMIA194US/JW202, and the National Key Research and Development Program of China under Grant No. 2017YFE0300405. Indirect support was provided under U.S. DoE Grant No. DE-FG02-08ER54999.

- ¹R. J. Fonck, P. A. Dupperex, and S. F. Paul, *Rev. Sci. Instrum.* **61**, 3487 (1990).
- ²S. F. Paul and R. J. Fonck, *Rev. Sci. Instrum.* **61**, 3496 (1990).
- ³G. McKee, R. Ashley, R. Durst *et al.*, *Rev. Sci. Instrum.* **70**, 913 (1999).
- ⁴Y. U. Nam, S. Zoletnik, M. Lampert *et al.*, *Rev. Sci. Instrum.* **83**, 10D531 (2012).
- ⁵H. J. Wang, Y. Yu, R. Chen *et al.*, *Rev. Sci. Instrum.* **88**, 083505 (2017).
- ⁶D. R. Smith, H. Feder, R. Feder *et al.*, *Rev. Sci. Instrum.* **81**, 10D717 (2010).
- ⁷A. R. Field, D. Dunai, R. Gaffka *et al.*, *Rev. Sci. Instrum.* **83**, 013508 (2012).
- ⁸S. Kado, T. Oishi, M. Yoshinuma *et al.*, *Rev. Sci. Instrum.* **81**, 10D720 (2010).
- ⁹I. H. Hutchinson, *Plasma Phys. Controlled Fusion* **44**, 71 (2002).
- ¹⁰N. L. Schoenbeck, S. D. Ellington, R. J. Fonck *et al.*, *Rev. Sci. Instrum.* **81**, 10D718 (2010).
- ¹¹N. Iwama, *J. Appl. Phys.* **50**(5), 3197–3206 (1979).
- ¹²J. M. Beall, Y. C. Kim, and E. J. Powers, *J. Appl. Phys.* **53**(6), 3933–3940 (1982).
- ¹³S. J. Levinson *et al.*, *Nucl. Fusion* **24**(5), 527 (1984).
- ¹⁴M. Jakubowski, R. J. Fonck, J. S. Kim, and G. McKee, *Rev. Sci. Instrum.* **70**, 874 (1999).
- ¹⁵G. R. McKee, C. Fenzi, R. J. Fonck *et al.*, *Rev. Sci. Instrum.* **74**, 2014 (2003).